Available online at www.sciencedirect.com
ScienceDirect
Proceedings of the Combustion Institute 33 (2011) 2937–2944
Proceedings of the Combustion Institute
www.elsevier.com/locate/proci

Turbulent flame speed for syngas at gas turbine relevant conditions

S. Daniele [a,*], P. Jansohn [a], J. Mantzaras [a], K. Boulouchos [b]

[a] Paul Scherrer Institut (PSI), Combustion Research Laboratory, 5232 Villigen PSI, Switzerland
[b] Swiss Federal Institute of Technology (ETH), Aerothermochemistry and Combustion Systems Laboratory Sonneggstr. 3, 8092 Zürich, Switzerland

Available online 7 August 2010

Abstract

Modifications of conventional natural-gas-fired burners for operation with syngas fuels using lean premixed combustion is challenging due to the different physicochemical properties of the two fuels. A key differentiating parameter is the turbulent flame velocity, S_T, commonly expressed as its ratio to the laminar flame speed, S_L. This paper reports an experimental investigation of premixed syngas combustion at gas turbine like conditions, with emphasis on the determination of S_T/S_L derived as global fuel consumption per unit time. Experiments at pressures up to 2.0 MPa, inlet temperatures and velocities up to 773 K and 150 m/s, respectively, and turbulence intensity to laminar flame speed ratios, u'/S_L, exceeding 100 are presented for the first time. Comparisons between different syngas mixtures and methane clearly show much higher S_T/S_L for the former fuel. It is shown that S_T/S_L is strongly dependent on preferential diffusive-thermal (PDT) effects, co-acting with hydrodynamic effects, even for very high u'/S_L. S_T/S_L increases with rising hydrogen content in the fuel mixture and with increasing pressure. A correlation for S_T/S_L valid for all investigated fuel mixtures, including methane, is proposed in terms of turbulence properties (turbulence intensity and integral length scale), combustion properties (laminar flame speed and laminar flame thickness) and operating conditions (pressure and inlet temperature). The correlation captures effects of preferential diffusive-thermal and hydrodynamic instabilities.

Keywords: Syngas combustion; Turbulent flame speed; High pressure; High inlet temperature; Lean premixed flame

1. Introduction

Lean premixed combustion represents the state-of-the-art gas turbine combustion technology for high efficiency and low emissions. This technology has been optimized for natural gas combustion and has demonstrated single-digit nitrogen oxides (NO_X) and very low carbon monoxide (CO) emissions (<20 ppm).

In recent times, integrated gasification combined cycle (IGCC) power plants have attracted increased attention, predominantly due to two reasons. The main driving force is the availability of diverse fuels, like biomass, coal, tars, etc. (sources of syngas), and the increasing concern for fuel supply security and flexibility, which prompt the use of syngas for high efficiency gas turbine-based power generation. A second reason is that syngas-based power plants facilitate cost-effective

* Corresponding author. Fax: +41 563102199.
E-mail address: salvatore.daniele@psi.ch (S. Daniele).

1540-7489/$ - see front matter © 2010 The Combustion Institute. Published by Elsevier Inc. All rights reserved.
doi:10.1016/j.proci.2010.05.057

carbon dioxide (CO_2) emissions reduction, when combined with fuel decarbonization.

The gasification of the aforementioned diverse fuels leads to a mixture, termed syngas, whose composition varies according to the gasification process and the original feedstock. Main fuel components in syngas are hydrogen (H_2) and CO, while diluents such as water (H_2O), nitrogen (N_2) or CO_2 can also be present in various amounts. These low-to-medium heating value gases are characterized by chemical and physical properties that can be drastically different from the ones of natural gas. High values of laminar flame speed (S_L), low density, high mass diffusivity and consequently low Lewis numbers (thermal over mass diffusivity), require different engine operating conditions for lean syngas combustion (so as to achieve a similar flame temperature with methane). The resulting effects on the turbulence-chemistry interactions portray a quite different combustion system when employing syngas fuels.

One of the most important parameters in premixed turbulent combustion is the turbulent flame speed (S_T), with its knowledge being of paramount importance for combustor design. The significance of mixture composition has been exemplified by Lipatnikov and Chomiak in their review [1], concluding that the turbulent flame speed is strongly affected by molecular transport: in fuel-lean syngas/air mixtures, transport effects are dominated by the H_2 component.

As reviewed in [2], in contrast to the extensive knowledge gained in the lasts decades for hydrocarbons (especially CH_4), very few experimental data are available in the literature for syngas fuels [3–5]. Moreover, the aforementioned data are not directly comparable due to the different adopted definitions for S_T, and the different experimental methodologies used. The lack of syngas data becomes very obvious especially when considering gas turbine relevant conditions, involving high pressures (1–3 MPa), high preheat temperatures (600–700 K) and high turbulence intensities ($u'/S_L > 50$).

The objective of this work is to describe turbulent combustion characteristics and in particular turbulent flame speeds for a variety of syngas-based fuel mixtures as function of equivalence ratio, pressure, inlet temperature and velocity, and turbulence intensity at gas turbine pertinent conditions.

2. Experimental setup, measuring techniques and data processing

Experiments are performed in a high pressure, optically accessible cylindrical combustion chamber (see Fig. 1) delivering a maximum thermal power of 400 kW. The chamber has a length of 320 mm with an inside diameter of 75 mm, and it is made of an air-cooled double-wall quartz tube (for more details, see [6]). The fuel/air mixture is delivered via a 25 mm diameter tube, coaxial to the reactor. The fuel is injected and mixed with electrically-preheated air 400 mm upstream of the combustion chamber. Fuel injection is accomplished in a co-flow configuration with the preheated air, through an array of five jets (1 mm in diameter) uniformly distributed within the delivery tube.

A sudden radial expansion by a factor of three between the delivery tube and the burner induces an outer recirculation zone which stabilizes the flame. There is no swirl or piloting flame applied. Pressurization is achieved by a cylindrical tank enclosing the reactor and delivery tube. Optical access to the reaction zone is provided by three quartz windows positioned on the tank, two side ones and one along the reactor axis (see Fig. 1).

Planar laser induced fluorescence (PLIF) of the OH radical was employed to assess the flame front position and turbulent flame speeds. The detailed laser/camera setup is described in [7] (excitation beam at 285 nm through the use of a pulsed Nd:YAG/dye laser system with 30 ns pulse duration, and fluorescence collection at 308 and 314 nm). The 285 nm PLIF light sheet entered the reactor counterflow, from the rear tank axial window. The raw images were post-processed adopting the methodology proposed in [8] with the modifications described in [5]. These modifications, introducing a local threshold methodology for the flame front location, were necessary to process PLIF images at high pressures and ultra-lean stoichiometries.

Measurements are reported in terms of parameters such as turbulent flame speed, S_T, flame length, F_L, and flame brush thickness, f_{BT}. Absolute values of S_T were derived by solving the continuity equation at the inlet section and at the average flame front surface [5]. The flame surface has been defined at a reaction progress variable of $\langle c\rangle = 0.05$, with c denoting OH signal intensity. Therefore, S_T represents a "volumetric, global fuel consumption rate" [2,9,10]. The flame length $F_L^{\langle c\rangle} = 0.05$ is defined as the axial distance between the combustor inlet and the position of the average flame front ($\langle c\rangle = 0.05$) along the centerline. Twice the difference of flame front positions at $\langle c\rangle = 0.50$ and $\langle c\rangle = 0.05$ defines the flame brush thickness, $f_{BT} = 2(F_L^{\langle c\rangle=0.50} - F_L^{\langle c\rangle=0.05})$.

For each operating condition, the final results (S_T, $F_L^{\langle c\rangle} = 0.05$, f_{BT}) are based on 400 images (instantaneous shots) acquired at a 20 Hz sampling rate. An S_T variation of up to ± 0.5 m/s has been observed for repeated measurements at any experimental condition. In general, it can be stated that high pressure/ultra-lean flames are characterized by a larger S_T uncertainty when compared to low pressure/less-lean flames. This is because high pressure and/or very lean mixtures

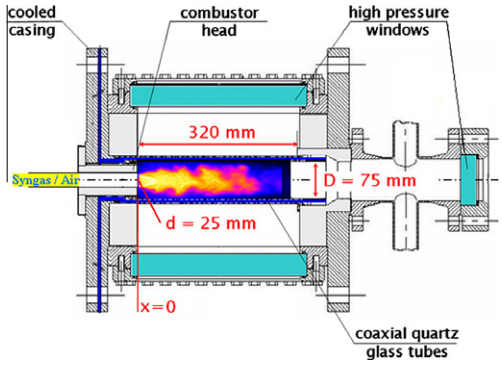

Fig. 1. Schematic of test rig.

Table 1
Composition of fuel stream (oxidizer stream is air).

Fuel	% vol.	Color
CH_4	100	Orange
CH_4 H_2 CO N_2	60–10–10–20	Gray
CH_4 H_2 CO	60–20–20	Black
H_2 CO	33–67	Green
H_2 CO	50–50	Red
H_2 CO	67–33	Brown
H_2 CO N_2	40–40–20	Blue

lead to a decrease in the PLIF intensity that in turn affects the quality of the results during the flame front detection procedure [5].

Flow field characteristics including turbulence intensity, u' and integral length scales, L_T have been measured in past works by particle image velocimetry, PIV [11].

Unstrained laminar flame speeds, S_L, were computed using the GRI 3.0 mechanism [12], while characterization of strained S_L will be reported in a future work. Table 1 provides the composition coding for Figs. 2, 4, and 7 and Table 2 the pressure coding for Figs. 2, 4, 6, and 7.

3. Results and discussion

3.1. Turbulent and chemical kinetic regimes of data set

Figure 2, positions the data of the present work in the Borghi diagram, as modified by Peters [13]. The bulk of the data fall in the thin reaction zones regime, a major part characterized by Damkholer numbers (Da) <1, with only a few data points in the broken reaction zones, characterized by Karlovitz number (Ka_δ) >1. For CH_4 no data could be acquired at $Da < 1$ as these flames encountered lean blow-out in this regime. In Fig. 2, l_m denotes the Zimont mixing scale [14].

Figure 3 provides OH-PLIF single-shot images at different equivalence ratios, Φ. An elongation

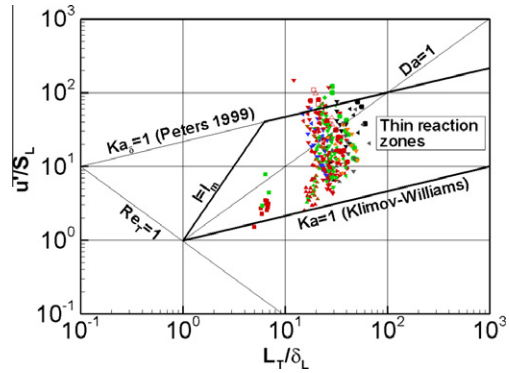

Fig. 2. Borghi diagram (modified by Peters) with data points acquired in this work. Karlowitz (Ka, Ka_δ), Damkholer (Da) and turbulent Reynolds (Re_T) numbers are based on integral length scale (L_T). Legend as in Table 2.

of the flame length is observed with decreasing Φ, while no differences in the flame morphology are evident when crossing $Da = 1$. The probability of a broken flame surface and the presence of burning isolated pockets increase with decreasing Φ. For $Ka_\delta > 1$ the reaction zone is broken; however, analysis of CO emissions at the exhaust confirms that combustion is still complete. Flame images for $Ka_\delta > 1$ have been processed with the same methodology, as it was always possible to define an average continuous reaction zone.

3.2. Relation between turbulent flame speed and flame front position

Recently [2,10,15], it has been stressed that turbulent flame speeds may depend on the geometry of the particular experimental rig, since local flame front wrinkles bear the memory of the ones generated upstream. In this respect, flames generated with similar geometries should preferably be compared. To eliminate most of the geometry dependence, we correlate turbulent flame speed values, S_T, with turbulence characteristics such as integral length scale, L_T, and turbulence intensity, u', measured under atmospheric-pressure, non-reactive flow conditions at the flame location.

The turbulent flow field in our configuration has been studied in the past [11]. Several experiments were conducted with different perforated plates mounted in the fuel/air mixing section. In the current study no perforated plates were used: it was impossible to position any element in the mixing section (which could act as potential flame holder) when firing syngas because of its high flashback propensity as described in more details in [16]. Previous studies have shown that the effect of different types of perforated plates on the turbulent flow field is only restricted to core flow regions close to the combustor inlet ($x < 2d$,

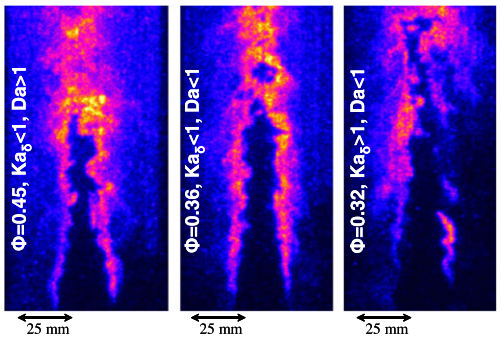

Fig. 3. OH-PLIF images corresponding to three different regimes.

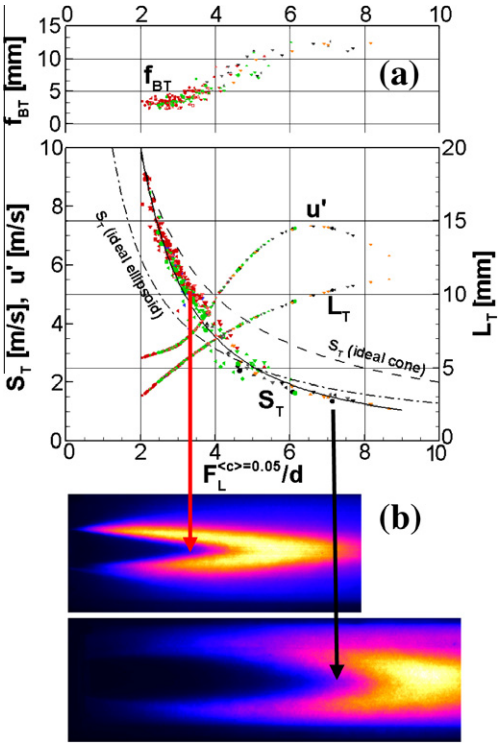

Fig. 4. (a) S_T, u', L_T, f_{BT} versus $F_L^{\langle c\rangle=0.05}/d$, and (b) averaged OH-PLIF images for two flames. Legend as in Table 2.

d = diameter of fuel/air delivery pipe), revealing that the turbulence field at the location of the flame front is essentially dominated by the shear-generated turbulence due to the backward facing step geometry [11]. Therefore, turbulence intensity and integral length scales were inferred in the present study by averaging over four different flow conditions corresponding to four perforated plate geometries. The resulting average values of u' and L_T on the combustor symmetry axis are presented in Fig. 4 versus the flame front position, $F_L^{\langle c\rangle=0.05}$ normalized by the injector diameter, d. The variation of the centerline u' in each of the four cases with respect to the average value, was at most 1 m/s. Centerline values are considered representative of the turbulence characteristics along the entire flame front: it has been shown that the flames stabilize along contours of nearly constant u' and L_T [11].

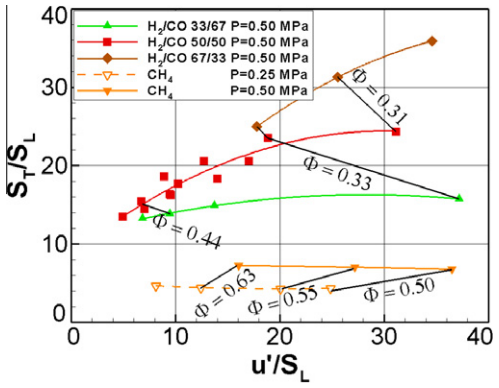

Fig. 5. S_T/S_L versus u'/S_L: H_2 content effect for syngas and pressure effect for CH_4.

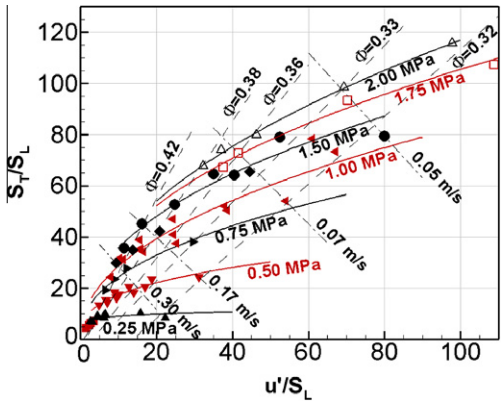

Fig. 6. S_T/S_L versus u'/S_L: pressure effect for syngas (50% vol. H_2/50% vol. CO). Legend as in Table 2. The dashed-dotted lines refer to constant S_L values.

Figure 4a presents a wide selection of S_T measurements comprising inlet temperatures from 423 to 773 K, equivalence ratios between 0.25 and 0.75, pressures from 0.1 to 2.0 MPa, and various fuel mixtures listed in Table 1. The strategy for the selection of these fuel compositions is detailed in [5]. In the same figure, f_{BT} values are also plotted.

The dashed and the dashed–dotted-lines in Fig. 4a represent S_T values corresponding to a flame with an ideal conical shape and to a rotationally-symmetric ellipsoid, respectively. The correlation between S_T and $F_L^{\langle c\rangle=0.05}$ is largely independent of gas mixture composition and operating conditions. "Short" flames assume conical

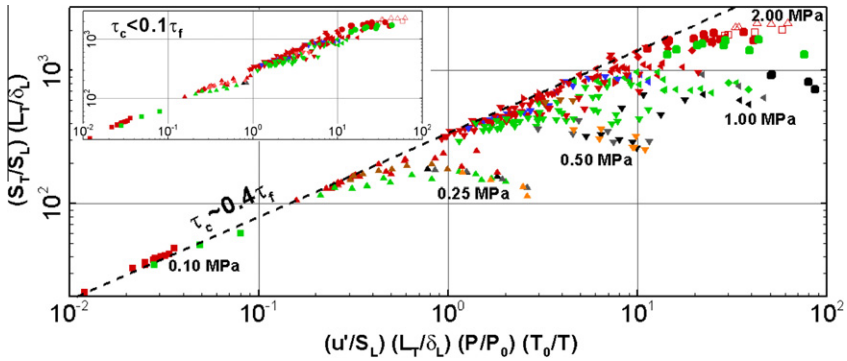

Fig. 7. Normalized turbulent flame speed data. Legend as in Tables 1 and 2.

Table 2
Legend for pressures.

Symbol	P (MPa)	Symbol	P (MPa)
■	0.10	♦	1.25
▲	0.25	●	1.50
▼	0.50	□	1.75
►	0.75	△	2.00
◄	1.00		

shapes, while "longer" flames rather resemble axisymmetric ellipsoidal shapes as depicted in Fig. 4b by the average OH-PLIF images (the arrows connect the data points to the corresponding flame locations, $F_L^{\langle c\rangle=0.05}$). Moreover, Fig. 4a, shows that the angle method used by Kobayashi [17] and other authors [4] for the determination of S_T, can lead for our combustor geometry to errors not only in the absolute value of S_T but also in the observed trends (see non-constant difference between the dashed and the solid lines). Venkateswaran et al. [4], using the same configuration as Kobayashi, reported an error by the angle method in estimating absolute values of S_T, stating however that trends were not affected. In direct contrast, Kobayashi showed no difference between values calculated with the angle method and the progress variable method ($\langle c\rangle = 0.1$) [18]. With the approach presented in this paper, it is possible to generate data at different u' (at the same inlet velocity) without varying the overall combustor geometry. The flame stabilizes at a certain location, where it encounters specific values of u' and L_T, according to its propagation capability.

Until now there are no values of global fuel consumption rate, S_T, reported in the literature for syngas compositions at high preheating temperatures, high pressures and high turbulence intensities. In [4], S_T (global consumption) values for only atmospheric-pressure and temperature are reported. A one-to-one comparison with this work is not possible as the conditions are different and the methodology used to post-process the data is also different.

3.3. Mixture composition effect on turbulent flame speed

Figure 5 reports measurements for a constant pressure of 0.5 MPa, $T_o = 623$ K and $U_0 = 40$ m/s for four different fuel mixtures. An additional dataset for CH_4 at 0.25 MPa is provided. Data points characterized by the same Φ are connected by additional solid lines.

It is well known that S_T/S_L values exhibit a first zone, for low values u'/S_L, wherein S_T/S_L is almost linearly proportional to u'/S_L, and a second zone where the S_T/S_L versus u'/S_L curve bends and appears to level-off as reviewed in [9]. The bending occurs for a particular u'/S_L depending on fuel mixture composition. Data for CH_4 have been apparently acquired within this second zone only.

The effect of pressure on S_T for CH_4 is depicted by the difference between the two data sets indicated with open and filled triangles. Increase in S_T/S_L with rising pressure has already been reported in [17,18]. This effect was attributed [17] to the growth of the hydrodynamic instability, DL, after Darrieus and Landau [19] who described this instability for laminar flamelets.

It is noted that Kobayashi's findings [17] were recently questioned by Lipatnikov and Chomiak [20], arguing that there is no evidence for the DL instability being alone responsible for the increase in S_T/S_L with rising pressure. Moreover, they concluded [1] that DL instability can be significant only for weak turbulence. The decrease of importance of DL effects at high u'/S_L is further supported by Peters [21], although he provided no insights on the impact of pressure. Therefore, the effect of DL instabilities at elevated pressures is still an open question.

Data at constant pressure confirm trends presented elsewhere at significantly lower u'/S_L and reviewed in [1]: the higher the H_2 content in the

mixture, the larger the S_T/S_L. This behavior can be attributed to preferential diffusive-thermal instability, PDT, as described in [1].

As u' in this work is taken at the flame front position along the centerline, and since u' varies upon Φ, it is not possible to acquire data at constant Φ and u'/S_L simultaneously. Therefore, we verified numerically that the Lewis number, Le_{H_2}, for every fuel mixture, does not change appreciably within the range of equivalence ratios presented, such that the difference in S_T/S_L for $P = 0.50$ MPa (Fig. 5) can be predominantly attributed to PDT effects due to different absolute H_2 levels in the mixture.

3.4. Pressure effect on turbulent flame speed

Figure 6 depicts data at different pressures (0.1–2.0 MPa) and various Φ (0.30–0.50), for a 50% vol. H_2/50% vol. CO composition. In addition, linear regression lines for constant Φ (dashed-lines) and constant S_L (dashed–dotted-lines) are shown. Regression lines for constant u' roughly follow the $\Phi =$ constant lines, and are thus not shown. This behavior is based on the experimental observation that the flame front position for constant Φ is only weakly affected by pressure, thus the reaction zone encounters roughly the same u' (see Fig. 4a).

An increase in pressure leads to an increase in S_T/S_L, irrespective of the way the pressure increase is attained (at constant u'/S_L, constant u', constant S_L, or constant Φ). This trend is similar to that reported for CH_4 [17] and also observed in the present data (Fig. 5). As a consequence, the phenomenological explanation for CH_4 [17], invoking the role of DL instability for the increase of S_T/S_L with pressure, could be considered valid for syngas as well, however, at higher u'/S_L. The increase in S_T/S_L with rising pressure is stronger when moving along a Φ isoline. In this case u' is also kept roughly constant, such that the increase in u'/S_L can be studied solely due to the decrease in S_L. Due to the decrease in S_L, for constant u' the flame front becomes more sensitive to hydrodynamic wrinkling, leading to the accelerated increase in S_T/S_L.

In case of syngas ($Le_{H_2} < 1$), we expect PDT effects to be important and to further discriminate data acquired at different pressures. To evaluate the role of PDT effects, we compare the S_T/S_L ratios at two pressures, 0.25 and 0.50 MPa for the syngas mixture presented in Fig. 6 and for the CH_4 in Fig. 5. Comparisons are performed within a range of u'/S_L (20–40) whereby S_T/S_L is weakly dependent on u'/S_L for syngas, and fairly independent for CH_4. These ratios are roughly 2.5 for syngas and 1.6 for CH_4. Hence, it appears that the syngas mixture undergoes an additional enhancement of S_T/S_L, most probably attributable to PDT and to the coupling between DL and PDT instabilities. The difference in these two factors cannot be attributed to the difference in laminar flame thickness; in fact, within the range of u'/S_L, considered for this comparison, the syngas mixture is characterized by a larger thickness, due to the smaller Φ (larger flame thickness reduces the possibility of flame wrinkling at small scales and does not contribute to an increase in S_T/S_L). An account for different flame thicknesses is addressed in the next section. A detailed description of the pressure effect on S_L alone has been reported in [16].

3.5. Correlation for normalized turbulent flame speed

Figure 7 reports a database of over 300 measured operating conditions (the data notation is given in Tables 1 and 2).

On the abscissa, the terms P/P_o and T_o/T account for pressure and inlet temperature variation (we chose: $P_o = 0.1$ MPa, $T_o = 1$ K, as in [22]). The term L_T/δ_L accounts for the capability of eddies having size between δ_L and L_T to wrinkle the flame front at a given u'; this term appears to also capture Lewis number effects via the dependence of δ_L on the thermal diffusivity.

A first data set, where S_T/S_L increases with a well-defined power law (proportional range, see insert), and a second one where S_T/S_L values level-off (bending range) can be distinguished. The bending occurs at u'/S_L values dependent on pressure, and not on mixture composition. The onset of bending is found to depend on the ratio of the following time scales:

$$\tau_f = \frac{L_T}{u'} \text{ and } \tau_c = \frac{f_{BT}}{S_T} \tag{1}$$

where τ_f is the turnover time of an eddy having the size of the integral length scale, thus representing the longest turbulent timescale interacting with the flame front; τ_c is the time necessary for the flame front to travel through the flame brush thickness, f_{BT}, thus denoting the timescale at which the flame can respond to flow perturbations.

Eddies characterized by τ_f much shorter than τ_c, have too high frequencies ($1/\tau_f$) to interact and contort the flame front, thus their contribution to the wrinkling process and consequently to the increase of S_T/S_L is meager or negligible. This concept was demonstrated in [23,24]. The criterion $\tau_c = 0.1\tau_f$ appears to be appropriate to separate the dataset in a "linear log–log" behavior (see insert in Fig. 7 and a "bending" one. As a matter of fact, this criterion ($\tau_c = 0.1\tau_f$) roughly corresponds to $S_T = u'$ (as it was found that $f_{BT} \sim 10L_T$).

The dashed-line in Fig. 7 describes the trend of those data in the "linear" range with comparable τ_f and τ_c ($\tau_c/\tau_f \approx 0.4$). Above this limiting line it

is not possible to find any data point: at these conditions, eddies can wrinkle the flame front apparently with maximum efficiency and no further wrinkling (i.e. acceleration of fuel consumption) is possible. A correlation for the dashed-line data in Fig. 7 can be written as:

$$\frac{S_T}{S_L} = a\left(\frac{u'}{S_L}\right)^{0.63}\left(\frac{L_T}{\delta_L}\right)^{-0.37}\left(\frac{P}{P_o}\right)^{0.63}\left(\frac{T}{T_o}\right)^{-0.63}; \quad a = 337.5 \tag{2}$$

The comparison of this correlation with other ones available in the literature leads to the following considerations:

1. A dependence of S_T/S_L on u'/S_L with a similar exponent ($n = 0.7$) was also reported by Klimov [25].
2. The negative exponent $n = -0.37$ of L_T/δ_L is not in contrast with other correlations [13,26]; for the data set supporting the above correlation, this term is related to P/P_o as:

$$\left(\frac{L_T}{\delta_L}\right) = b\left(\frac{P}{P_o}\right)^{0.66}; b = 8.3 \tag{3}$$

By substituting Eq. (3) in (2), the exponent of L_T/δ_L appears to be positive (0.58), in agreement with the previous mentioned correlations [13,26].

3. Kobayashi [18,27] has proposed similar correlations, accounting just for the pressure ratio. We also attempted simpler correlations by plotting S_T/S_L versus $(u'/S_L)(P/P_o)(T_o/T)$, not reported here for brevity. This correlation produced also good results; however data points characterized by large differences in L_T/δ_L were not correlating on a single straight line as in Fig. 7 but on parallel lines having roughly the same exponent, with proportionality coefficients being higher for lower pressures. These differences were particularly obvious for data at 0.1 MPa (as depicted by Fig. 2), which are characterized by much smaller L_T/δ_L. In [18,27], Kobayashi obtained a correlation for S_T/S_L versus $(u'/S_L)(P/P_o)$ with pressure power laws having exponents $n = 0.38$ and 0.40. These measurements were performed within the corrugated flamelets regime. Working out the global exponent, n, in P/P_o by substituting again Eq. (3) in (2), we obtain $n = 0.385$. The agreement with [18,27] is seen as a confirmation that there is no experimental evidence that the two regimes (corrugated flamelets and thin reaction zones) differ when comparing the S_T, as observed in [1].

4. Conclusions

Lean premixed turbulent flames were investigated at gas turbine relevant conditions. Extensive measurements were performed for a variety of syngas mixtures and for methane. Measurements were mainly conducted in the thin reaction zones regime. For the first time, experimental turbulent flame speed data were reported for syngas at pressures up to 2.0 MPa, preheat temperatures up to 773 K and $u'/S_L > 100$. In contrast to many other works, S_T in terms of global consumption has been related to the turbulence properties measured at the flame front and not at the inlet section, so as to minimize the dependence of this parameter on the geometrical characteristics of the burner.

The dependence of S_T/S_L on H_2 content in the fuel mixture and on pressure was assessed. The increase of S_T/S_L on H_2 content was attributed to preferential diffusive-thermal (PDT) effects, being active also at high turbulence intensity. These effects have been seen to also play a role in the increase of S_T/S_L with pressure, attributed to the coupling of PDT with hydrodynamic instabilities.

Syngas S_T/S_L versus u'/S_L data show linear and bending characteristics, similar to that known for CH_4. The onset of bending depends on the ratio between the integral length scale eddy turnover time and the timescale at which the flame front can react to flow perturbations. The latter was expressed as the ratio of the flame brush thickness to S_T. A correlation for S_T/S_L independent on the fuel mixture composition, (apparently) capable of capturing both hydrodynamic and preferential diffusive-thermal instabilities has been proposed.

Acknowledgments

We gratefully acknowledge financial support of this research by the Swiss Federal Office of Energy (BFE) and Alstom Power Switzerland, and thank Dr. Rolf Bombach, Dr. Wolfgang Kreutner, Dr. Alexey Denisov and Mr. Daniel Erne for supporting the experimental campaign.

References

[1] A. Lipatnikov, J. Chomiak, *Prog. Energy Combust. Sci.* 31 (2005) 1–73.
[2] R.K. Cheng, *Synthesis Gas Combustion – Fundamentals and Applications*, CRC Press, Roca Raton, London, New York, 2009, pp. 129–168.
[3] R.K. Cheng, D. Littlejohn, P.A. Strakey, T. Sidwell, *Proc. Combust. Inst.* 32 (2009) 3001–3009.
[4] P. Venkateswaran, D. Marshall, D.R. Noble, J. Antezana, J.M. Seitzman, T.C. Lieuwen, *Global turbulent consumption speeds ($S_{T,GC}$)* of H_2/CO blends, Proc. ASME Turbo Expo 2009, Orlando, Florida, 2009.
[5] S. Daniele, P. Jansohn, K. Boulouchos, *Flame front characteristic and turbulent flame speed of lean premixed syngas combustion at gas turbine relevant conditions*, Proc. ASME Turbo Expo 2009, Orlando, Florida, 2009.

[6] P. Griebel, E. Boschek, P. Jansohn, *J. Eng. Gas Turb. Power-Trans. ASME* 129 (2007) 404–410.
[7] P. Griebel, R. Bombach, A. Inauen, W. Kreutner, R. Schären, *Structure and NO emission of turbulent high pressure lean premixed methane/air flames*, Sixth European Conference on Industrial Furnaces and Boilers, INFUB, 2002, pp. 45–54.
[8] P. Griebel, P. Siewert, P. Jansohn, *Proc. Combust. Inst.* 31 (2007) 3083–3090.
[9] A. Lipatnikov, J. Chomiak, *Prog. Energy Combust. Sci.* 28 (2002) 1–74.
[10] J.F. Driscoll, *Prog. Energy Combust. Sci.* 34 (2008) 91–134.
[11] P. Siewert, *Flame Front Characteristics of Turbulent Premixed Lean Methane/Air Flames at High-pressure and High-temperature*, Ph.D thesis, Swiss Federal Institute of Technology ETH-Zurich, Zurich, Switzerland, 2005, available at <http://e-collection.ethbib.ethz.ch/ecol-pool/diss/fulltext/eth16369.pdf>.
[12] G.P. Smith, D.M. Golden, M. Frenklach, et al., available at <http://www.me.berkeley.edu/gri_mech/>.
[13] N. Peters, *J. Fluid Mech.* 384 (1999) 107–132.
[14] V.L. Zimont, *Combust. Explo. Shock Waves* 15 (1979) 305–311.
[15] I.G. Shepherd, R.K. Cheng, *Combust. Flame* 127 (2001) 2066–2075.
[16] S. Daniele, P. Jansohn, K. Boulouchos, *Flash back propensity of syngas flames at high pressure: diagnostic and control*, Proc. ASME Turbo Expo 2010, Glasgow, UK, 2010.
[17] H. Kobayashi, K. Tamura, K. Maruta, T. Niioka, F.A. Williams, *Proc. Combust. Inst.* 26 (1996) 389–396.
[18] H. Kobayashi, K. Seyama, H. Hagiwara, Y. Ogami, *Proc. Combust. Inst.* 30 (2005) 827–834.
[19] L. Landau, *Acta Physicochim. Urss* 19 (1944) 77–85.
[20] A. Lipatnikov, J. Chomiak, *Prog. Energy Combust. Sci.* 36 (2010) 1–102.
[21] N. Peters, H. Wenzel, F.A. Williams, *Proc. Combust. Inst.* 28 (2000) 235–243.
[22] M. Metghalchi, J.C. Keck, *Combust. Flame* 38 (1980) 143–154.
[23] W.T. Ashurst, G.I. Sivashinsky, V. Yakhot, *Combust. Sci. Technol.* 62 (1988) 273–284.
[24] J. Mantzaras, *Combust. Sci. Technol.* 86 (1992) 135–162.
[25] A.M. Klimov, *Laser React. Syst.* 88 (1983) 133–146.
[26] V. Zimont, W. Polifke, M. Bettelini, W. Weisenstein, *J. Eng. Gas Turb. Power-Trans. ASME* 120 (1998) 526–532.
[27] H. Kobayashi, Y. Kawabata, K. Maruta, *Proc. Combust. Inst.* 27 (1998) 941–948.